Ordering Transitions of Fluoroalkyl-Ended Poly(ethylene glycol): Rheology and SANS

Giyoong Tae,[†] Julia A. Kornfield,*[,†] Jeffrey A. Hubbell,[‡] and Jyotsana Lal[§]

Division of Chemistry and Chemical Engineering, 210-41, California Institute of Technology, Pasadena, California 91125; Institute for Biomedical Engineering and Department of Materials, ETH-Zurich and University of Zurich, 8044 Zurich, Switzerland; and IPNS, Argonne National Laboratory, Argonne, Illinois 60439

Received October 18, 2001; Revised Manuscript Received March 6, 2002

ABSTRACT: Aqueous solutions of associative polymers consisting of poly(ethylene glycol) (PEG) (6K or 10K g/mol) terminated at both ends with hydrophobic fluoroalkyl segments, $-(CH_2)_2C_nF_{2n+1}$ ($n = 6$, 8, or 10), exhibit ordering transitions with increasing concentration. The hydrophobic cores of the micelle-like aggregates order into a body-centered-cubic (bcc) structure, as observed by small-angle neutron scattering. The aggregation number of the hydrophobic core N_{ag} is determined by the length of the hydrophobic end group and is insensitive to polymer concentration or temperature. Ordering is enhanced by reducing PEG length for a given end group (hence, similar N_{ag}) or by increasing end group length (larger N_{ag}) for a given PEG length. This micelle packing effect is manifested in changes in the viscoelastic properties. Specifically, the single-relaxation behavior in the dynamic moduli changes upon ordering as a new low-frequency elastic plateau appears, and in creep a linear response changes to yielding behavior.

Introduction

Poly(ethylene glycol)s (PEGs) modified with hydrophobes at both ends have been investigated widely as model associative polymers.[1−22] The ability to tune their properties by choice of PEG length and hydrophobe provides the basis for applications as associative thickeners,[1,2,12] sieving media for DNA sequencing,[4,5] and in-situ forming gels for controlled release.[23] Most of the systems studied so far do not exhibit a first-order phase transition from sol to gel but form a single phase over the entire concentration range.[4−13,19−21] However, a first-order transition (i.e., sol−gel coexistence) has been observed for PEGs modified with sufficiently hydrophobic ends, long alkyl groups (C12 on PEG 2K or 4K g/mol,[17] C16 or C18 on PEGs of 20K or 35K g/mol[14−16]), or fluoroalkyl groups (C6, C8, or C10 on PEG of 6K or 10K g/mol).[22] This phase separation was predicted by Semenov et al., who anticipated a gas−solid-like transition with a dilute phase of micelles and free chains ("gas") in equilibrium with a close-packed phase of micelles ("solid").[24] On the basis of the lyotropic transitions observed in micelles,[25−28] polymer surfactants,[29−35] and star polymers,[36] ordering of associative polymers into a solidlike phase of micelles is quite plausible but has only been reported in a few cases (2K and 4K PEG with C12 alkyl ends[17] and 10K PEG with C8 fluoroalkyl ends[19]). Alternatively, Pham et al. advanced a view in which the coexisting phases are a "gas" and a condensed "liquid" of micelles.[15] Both theories indicate that the phase behavior (continuous vs first-order sol−gel transition) is determined by the aggregation number of the hydrophobic cores, N_{ag}, which controls the exchange entropy gained by formation of a dense phase.

Experimental examination of the relationship between single-phase vs sol−gel coexistence behavior and N_{ag} has been limited by the difficulty in establishing N_{ag}. Aggregation numbers for hydrocarbon ends have been measured by several research groups and range between 20 and 80 (summarized in Table 2 of ref 15), with substantial discrepancies among results even for fixed polymer structure. For fluorocarbon end groups, there are only three reports with disparate findings. For comparable PEG lengths (5K monofunctional, 10K telechelic), dimeric association ($N_{ag} = 2$) was reported[39,40] for a C6 fluoroalkyl ($C_6F_{13}C_2H_4-$), whereas a large aggregation number ($N_{ag} \sim 100$) was found[19] for a C8 fluoroalkyl ($C_8F_{17}C_{11}H_{22}-$). For a much longer PEG length (35K), aggregation numbers of 20 for C6 and 30 for C8 end groups were observed.[6] In contrast to the literature on block copolymers,[26−35] there have been few studies[6,7,16] that connect the self-assembled nanostructure (e.g., N_{ag}, $S(q)$)[17,19] to viscoelastic properties[10,12,13] of associative polymers.

The rheological studies of model associative polymer systems have focused mainly on alkyl-ended PEGs that show single-phase behavior.[10−13] They are almost perfect Maxwell (single relaxation time) fluids. The flow curve (viscosity vs shear rate) consists of three regimes: a shear-rate-independent region at low shear rates, a modestly shear thickening region at moderate shear rates, and a shear thinning region at high shear rates. The few alkyl-ended systems that exhibit sol−gel coexistence (35K g/mol PEG with C16 and C18 hydrocarbon end groups) also show single relaxation behavior in the "gel".[16] Motivated by the stronger hydrophobicity of fluoroalkyl groups, PEGs modified with fluorocarbon ends have also been examined. Prior studies reported only materials that exhibit single-phase behavior and found essentially the same characteristics as the hydrocarbon systems,[4−6,18] except for the disappearance of shear thickening.[6]

Our focus is on PEGs with fluoroalkyl ends, due to their potential in biomedical applications as in-situ forming hydrogels: associating polymers that exhibit coexisting sol and gel phases exhibit "surface erosion"

[†] California Institute of Technology.
[‡] University of Zurich.
[§] Argonne National Laboratory.
* Corresponding author: Tel 626 395 4138; Fax 626 568 8743, e-mail jak@cheme.caltech.edu.

10.1021/ma011809e CCC: $22.00
Published on Web 04/27/2002

Table 1. Modified R_f-PEGs

sample	PEG block (kg/mol)	modified end(s)	end group[a]	conv[b] (%)
20KC8	20	2	$-C_8F_{17}$	96
20KC10		2	$-C_{10}F_{21}$	97 (92)
10KC8	10	2	$-C_8F_{17}$	94
10KC10		2	$-C_{10}F_{21}$	94 (96)
6KC6	6	2	$-C_6F_{13}$	99
6KC8[c]		2	$-C_8F_{17}$	89
6KC10		2	$-C_{10}F_{21}$	97 (97)
5KmPC8	5	1	$-C_8F_{17}$	89
5KmPC10		1	$-C_{10}F_{21}$	91

[a] Full end group is $-\text{IPDU}-(CH_2)_2-C_nF_{2n+1}$, where IPDU is

[b] Degree of substitution as determined by ^{19}F NMR (selected values determined by HPLC are in parentheses), as described in ref 20. [c] A small amount of material with higher end group conversion (95%) was also prepared for comparison (see text).

characteristics that are attractive for controlled release, tissue engineering, and other biomedical/biotechnology applications.[22] By spanning a wide range of PEG lengths and fluoroalkyl lengths, we make the connection between molecular structure and self-assembled structure of the gel, rheological responses, and the aggregation state of the hydrophobes (aggregation number of the fluoroalkyl ends). Here we report an abrupt rheological transition from single relaxation behavior to solidlike behavior with increasing concentration, which has not been reported for associative thickeners or hydrophobically modified PEG micelles (single-ended). Using SANS, we show that this rheological transition correlates with ordering into a bcc phase, analogous to the viscoelastic signatures of ordering into to cubic phases in block copolymer solutions.[26] The aggregation number of the hydrophobic cores is determined using a combination of telechelic and monofunctional chains, leading to the conclusion that the aggregation number is determined by fluoroalkyl length, insensitive to concentration, temperature, and PEG length. In contrast to theoretical predictions, the phase behavior does not correlate in a simple way with aggregation number but instead shows strong effects of PEG length.

Experimental Section

Synthesis of PEGs with Fluorocarbon End Groups (R_f-PEGs). Poly(ethylene glycol) (PEG) of nominal molecular weights 6K, 10K, and 20K g/mol were end group modified with fluorocarbon ends ($-C_yF_{2y+1}CH_2CH_2$, y = 6, 8, or 10) using diisocyanate linkage. Syntheses and characterizations were done as described previously.[22] The samples prepared for this study are described in Table 1, where *x*KC*y* is a polymer with a PEG midblock that is *x* kg/mol and with *y*-carbon fluoroalkyl end groups, $C_yF_{2y+1}CH_2CH_2$. Similarly, *x*KmC*y* is a monofunctional R_f-PEG prepared using *x* kg/mol PEG methyl ether, therefore having a *y*-carbon fluoroalkyl hydrophobe only at one end.

Rheological Measurements. In a vial, weighed amounts of dried bifunctional PEG-R_fs were dissolved in deionized water and mechanically shaken. The mixing time was adjusted so that the solution reached equilibrium, as inferred from the disappearance of any visible turbidity. The prepared samples were centrifuged before loading to remove entrapped bubbles. A stress-controlled rheometer (SR 5000, Rheometric Scientific) equipped with a solvent trap was used with a cone-and-plate geometry (0.1 rad cone angle and 25 mm diameter) for rheological measurements. Evaporation from the sample restricts measurement temperature and time. With the appropriate solvent trap, drying of the sample was negligible for 12 h at 25 °C, but at higher temperatures, the drying effect was noticeable after a few hours. Drying is also unavoidable during the loading of the sample on the rheometer, which takes 5−10 min. So, the actual concentration of the sample might be slightly higher than indicated. All data shown in the figures are for experiments performed at 25 °C, unless otherwise indicated, and the reference temperature for time−temperature superposition is also 25 °C. Sample loading is achieved by lowering the upper part of sample holder (cone) slowly after placing the sample at the center of the bottom plate. Then, the sample is trimmed to match the diameter of the cone. The sample is allowed to reequilibrate after loading. Prior to rheological testing, the approach to equilibrium is monitored using small strain dynamic shear (~2% at 1 rad/s), applied until no appreciable change of modulus is observed (typically 2 h or less).

Table 2. Phase Behavior of Bifunctional R_f-PEGs

sample	type of phase behavior	equilibrium compositions in water (25 °C) $C_{gel,eq}$[a] (wt %)	$C_{sol,eq}$[b] (wt %)
20KC8	1 phase	N/A	N/A
20K10	1 phase	N/A	N/A
10KC8	2 phase	6.5 ± 0.2	0.075 ± 0.005
10K10	2 phase	6.8 ± 0.7	0.019 ± 0.008
6KC6	2 phase	9.5 ± 0.5	0.066 ± 0.007
6KC8	2 phase	11.0 ± 0.3	0.042 ± 0.007
6KC10	insoluble	N/A	N/A

[a] Equilibrium gel phase concentration. [b] Equilibrium sol phase concentration.

SANS Measurements. Samples were dissolved in D_2O (over a period of several days at 37 °C) at various concentrations and loaded into closed, quartz sample holders of 2 mm thickness. Each sample was annealed at 45 °C (typically for 12 h) and then reequilibrated to ambient temperature (>1 h) before loading into the temperature-controlled stage. Measurements were performed in time-of-flight mode in the small-angle diffractometer (SAD) beamline at the Intense Pulsed Neutron Source (IPNS) in Argonne National Laboratory (Argonne, IL) with 0.005 Å < q < 0.7 Å. At each experimental temperature, the sample was allowed to equilibrate for 1 h and held isothermally during acquisition. The acquisition times were 30 min for most samples and 5 h for the dilute (0.5 wt %) samples of monofunctional R_f-PEGs.

Results

Phase Behavior.[22] The phase behavior of bifunctional R_f-PEGs is governed by the relative length of the PEG midblock and the fluoroalkyl end groups (Table 2). 6KC10 does not exist as a homogeneous phase in water but rather exists only as a slightly swollen precipitate. At the other extreme, 20KC10 and 20KC8 exist as homogeneous solutions over the whole range of concentration. Polymers that lie in between in terms of the relative length of PEG to R_f (for example, 6KC6, 6KC8, 10KC8, and 10KC10) show phase separation into a gel coexisting with a sol. The two-phase character of 6KC8 may offer an explanation of the surprising lack of viscosity enhancement reported for a similar polymer:[18] if the state of the sample under steady shear was a dispersion of gel particles suspended in sol, the viscosity would remain close to that of the sol phase.

The equilibrium gel phase concentration ($C_{gel,eq}$) varies inversely with PEG midblock length and is insensitive to R_f length (Table 2). The phase boundary is almost temperature-invariant, but some increase of the gel phase concentration was observed for 10KC8 above 60 °C. These characteristics agree with previously reported hydrocarbon-ended phase-separating systems.[15] The sol

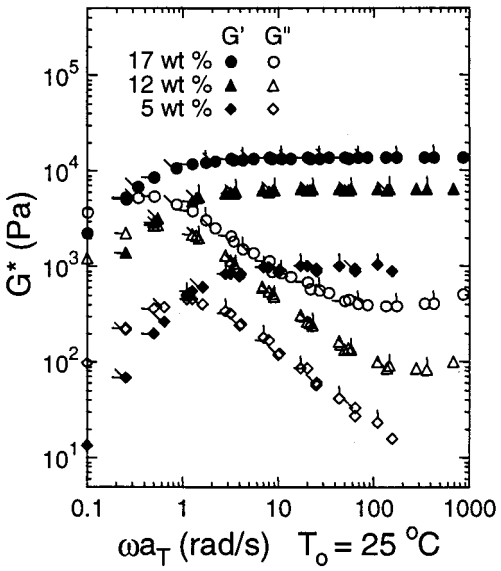

Figure 1. Dynamic moduli of 20KC10 solutions (temperatures are distinguished using pip marks: left, 25 °C; upper-left, 17 °C; up, 19 °C; and none, 1 °C).

phase concentrations are very small for all samples (<0.1 wt %), and unlike observed for the gel composition, the end group length as well as the PEG length affects the equilibrium sol concentration.

Linear Viscoelastic Properties of Non-Phase-Separating Species. The single-phase systems, e.g., 20KC10, show nearly single relaxation behavior for all concentrations in the range tested (from 5 to 17 wt %) (Figures 1 and 7a, taken together).[41] The relaxation time is associated with the end group dissociation time,[3−21,53] here denoted $\tau_{e.d.}$. With increasing concentration (up to 17 wt %), the plateau modulus at high frequency (G_∞) increases quadratically and the relaxation time increases linearly (Figure 2).[16] In steady shear, the flow curve shows only the plateau and shear thinning regimes (shear thickening is not found).[6] These observations agree with the general characteristics of previously examined fluorocarbon-ended systems.[4−6,18] As concentration increases (>10 wt %), an upturn of G'' at high frequency (Figure 1) is observed, as has been observed in single-phase-type hydrocarbon-modified PEG.[7,42]

Linear Viscoelastic Properties of Gels for Sol−Gel Coexisting Species. At their equilibrium gel concentrations, sol−gel coexisting systems are described by a single relaxation behavior, like the single-phase systems.[4−6,10,16,22] The end group length largely determines the relaxation time: increasing the R_f length from C8 to C10 produces a large change (~40-fold) in $\tau_{e.d.}$, while changing PEG length for fixed end groups has little effect on $\tau_{e.d.}$.[22] The PEG midblock determines G_∞ of the gel phase: a similar value in G_∞ is observed for 10KC10 and 10KC8 (~10^4 Pa, Figure 3) at their $C_{gel,eq}$, reflecting the similar density of physical junctions in these gels, evident from the similar values of their equilibrium swelling ratios (Table 2). A higher value of G_∞ is observed for 6KC8 at $C_{gel,eq}$ (Figure 3), indicating that a higher density of physical junctions is present, which agrees with its smaller swelling ratio compared to 10KC10 and 10KC8 (Table 2).

At concentrations higher than their sol−gel coexistence concentration, a new plateau (G_L) appears in the low-frequency regime. For 10KC8, this new plateau develops with increasing concentration from 8 to 12%;

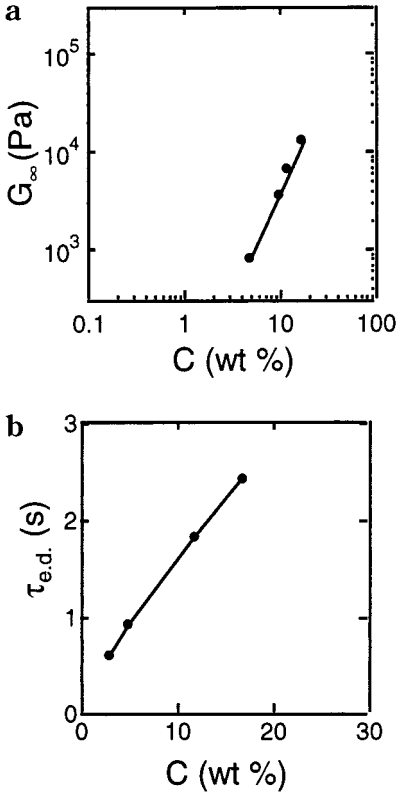

Figure 2. Concentration dependence of material properties of 20KC10 solutions: (a) high-frequency plateau modulus and (b) relaxation time end group dissociation mode ($\tau_{e.d.}$).

above 11 wt %, G' and G'' do not cross in the frequency window tested (Figure 4). The new plateau is not observed immediately after loading the sample in the rheometer. During loading, a significant deformation is exerted on the sample, after which the equilibrium state gradually recovers (Figure 5). Initially, terminal behavior is observed, followed by the development of the low-ω plateau. For 10KC8 at 12 wt % concentration, this change is almost complete in 4 h, observed with ~2% strain at 1 rad/s. This new plateau extends below 0.01 rad/s, and G' and G'' seem to cross around 0.001 rad/s at 25 °C for 12 wt % solution of 10KC8 (Figure 6), on a time scale 4 or 5 orders of magnitude slower than $\tau_{e.d.}$ (Figure 4).

As the temperature increases, the magnitude of G_L is reduced. Thus, time−temperature superposition fails (Figure 6). For 10KC10, this new plateau occurs at somewhat lower concentration than that of 10KC8. Above 10 wt %, G' and G'' no longer cross over each other. In the case of 6KC8, this change occurs for concentrations only slightly greater than $C_{gel,eq}$: for a specimen with 89% substitution of the ends (6KC8 in Table 2), the low-ω plateau is observed at 12 wt % at relatively low temperature (<9 °C). Another sample with a higher conversion of the ends (~95% substitution) shows the low-ω plateau at 12 wt % even at 25 °C.

Comparison of R_f-PEG to Bare PEG. Solutions of PEG homopolymers of 6K, 10K, and 20K g/mol in the concentration range tested above show negligible viscoelasticity compared to their fluoroalkyl-modified analogues. Thus, it may be concluded that the observed viscoelastic responses result from the association of the hydrophobic groups.

Creep Behavior. Qualitatively different creep behavior was observed for the single-relaxation time

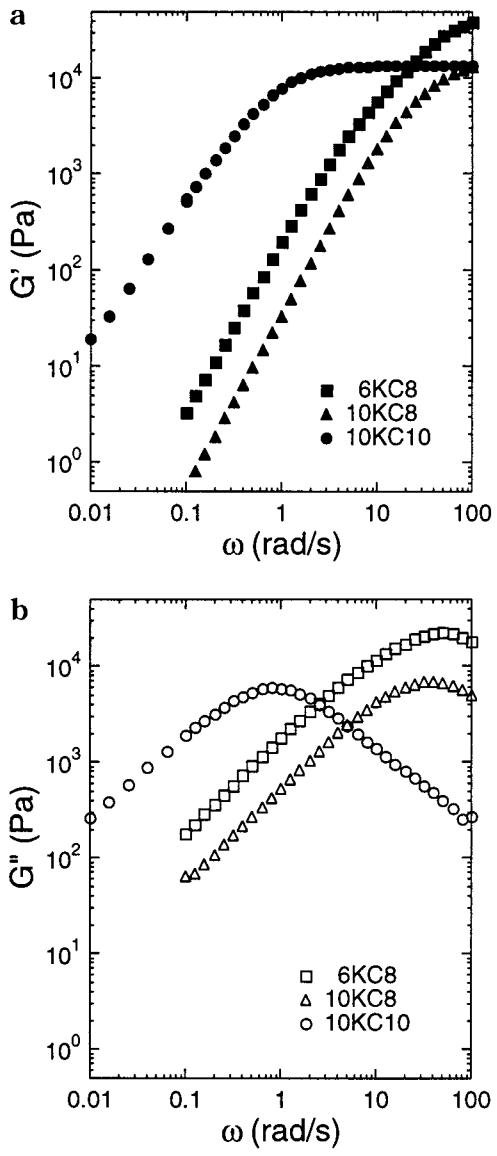

Figure 3. Dynamic moduli of the gel phases at the equilibrium gel concentrations ($C_{gel,eq}$) of the sol−gel coexisting species at 25 °C: (a) storage modulus and (b) loss modulus.

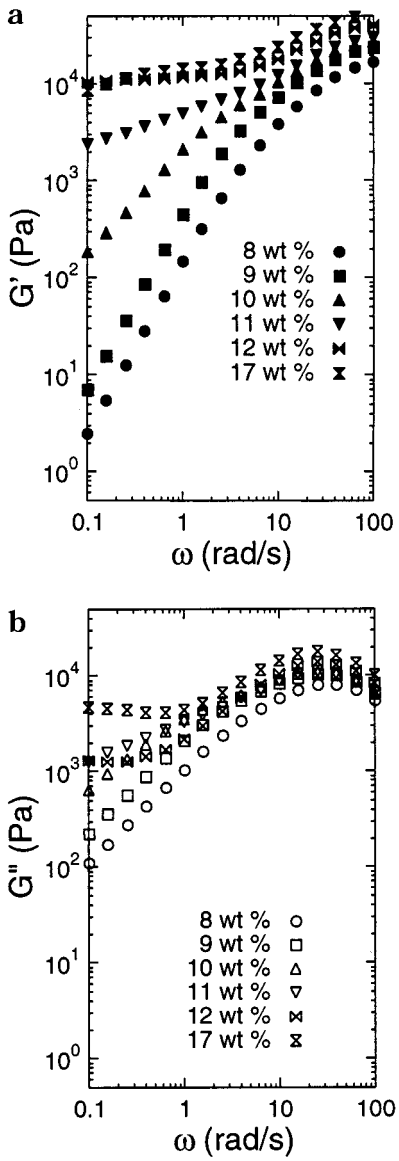

Figure 4. Dynamic moduli of 10KC8 solutions at $C > C_{gel,eq}$ at 25 °C: (a) storage modulus and (b) loss modulus.

samples vs those with the extended, low-ω plateau (G_L) (Figure 7). In response to a constant applied stress, the single-phase system 20KC10 behaves like a Maxwell fluid: the strain grows nearly linearly (Figure 7a), and the compliance $J(t) = \gamma(t)/\sigma$ is independent of stress from 10 to 100 Pa. These characteristics accord well with linear response, in view of the dynamic moduli of 20KC10 (Figures 1 and 2). Furthermore, $J(t)$ is very reproducible, even when successive experiments are performed with a short time in between (a few minutes). The solutions of sol−gel coexisting species near $C_{gel,eq}$ (the single-relaxation time samples) also show a linear growth of strain from the beginning of the creep experiment (data not shown).

In contrast to the samples that have single-relaxation behaviors, the solutions that have a low-ω plateau show a transition from a gradual creep (e.g., roughly $J(t) \sim t^n$ with $n \sim 0.13$ for 10KC8) initially to viscous flow at long time (10KC8 in Figure 7a). Decreasing PEG length (cf. 6KC8 and 10KC8 in Figure 7a) increases the initial resistance to creep and shifts the transition to viscous flow to higher stress and longer time (500 Pa is not sufficiently large for 6KC8 to show viscous flow behavior in 30 min, Figure 7a). Increasing fluoroalkyl length (cf. 10KC8 in Figure 7a to 10KC10 in Figure 7b) also makes the gel stiffer and delays the transition to viscous flow. The initial very slow creep is insensitive to the applied stress (Figure 7b); however, the time at which the viscous flow regime emerges and the magnitude of the viscosity both decrease with increasing stress. The distinctive shape of $J(t)$ for 10KC10—initial creep, then an elastic plateau, then viscous flow—is reminiscent of the behavior of certain ordered micellar solutions.[43]

Like the memory effect following samples that have a low-ω plateau loading (Figure 5), following a given creep experiment (reaching strain >5%), a subsequent creep experiment leads to a different $J(t)$ as a function of the resting time allowed between the two experiments. The time scale for fully recovering the initial creep response is similar to that required to recover the low-ω plateau after loading (several hours).[44] Thus, the formation of the new elastic plateau in the dynamic moduli is correlated with the "yielding behavior" of the samples in creep tests.

Lyotropic Ordering of the Gel Phase. To examine whether micelle packing is responsible for the develop-

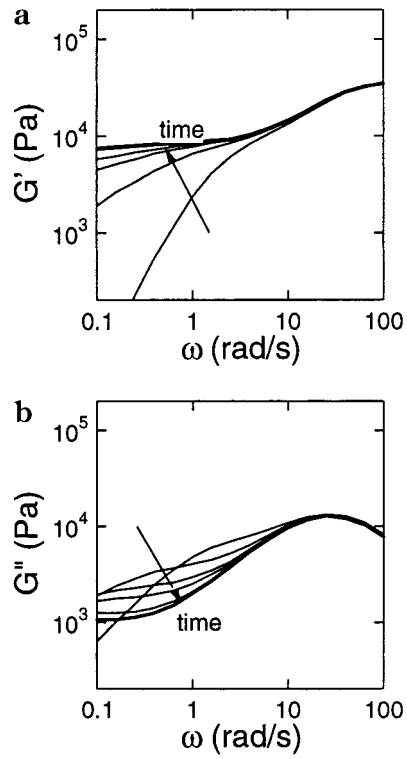

Figure 5. Development of the low-frequency plateau with time after loading (see text), illustrated by 10KC8 at 12 wt % and at 25 °C: (a) storage modulus and (b) loss modulus. Dotted curve recorded immediately after loading; successive curves recorded at 1 h intervals.

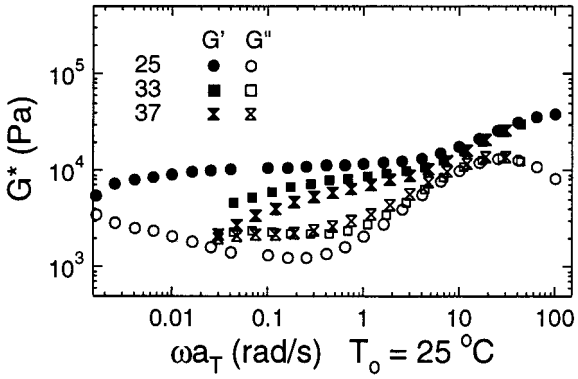

Figure 6. Dynamic moduli of 10KC8 12 wt % solution at various temperatures, shifted so that their end group dissociation modes superimpose.

ment of the low-ω plateau, SANS measurements were performed. The scattering pattern originating from the ordering of the hydrophobic cores of the micelles is observed as a primary peak. This peak becomes sharper and shifts to higher wave vector, q, with increasing concentrations (Figure 8), indicating improved long-range order and a decrease in the lattice spacing. The emergence of low-ω plateau in the storage modulus with increasing concentration correlates with the formation of the ordered structure; increase in G_L correlates with stronger ordering (cf. Figures 4 and 8).

Increasing temperature decreases the degree of ordering (Figure 9). However, the peak position does not change with temperature, which implies that the aggregation number of the hydrophobic cores does not change in the temperature range tested (25−49 °C). Thus, the decrease in G_L with increasing temperature

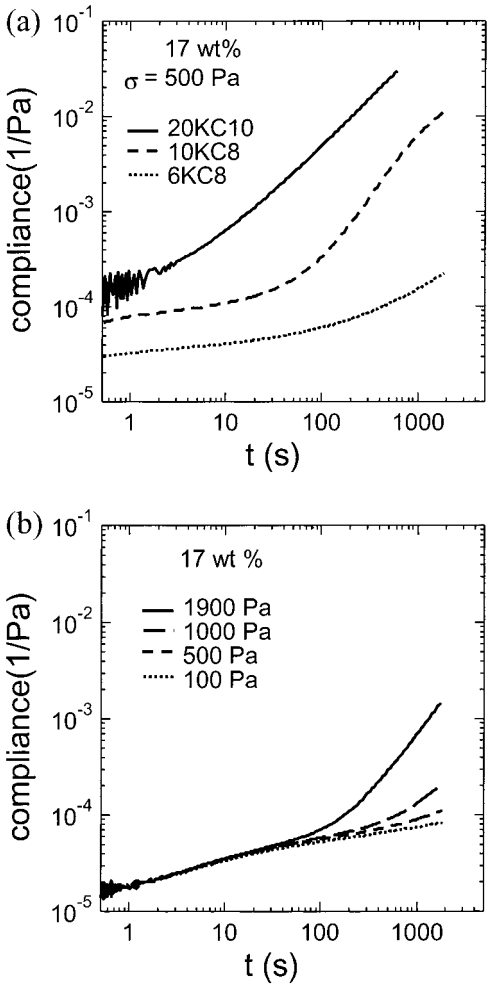

Figure 7. Creep responses (a) as a function of molecular structure for fixed concentration (17 wt %, σ = 500 Pa) and (b) as a function of applied shear stress (for 10KC10 17 wt %).

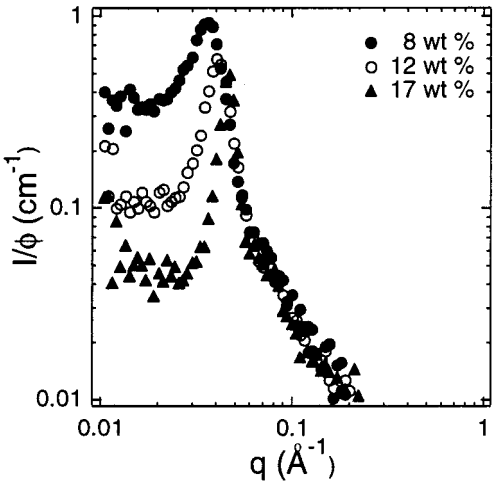

Figure 8. SANS pattern of 10KC8 solutions as a function of concentration at 25 °C.

(Figure 6) can be understood in terms of softening of the ordered lattice.

At fixed concentration, very different ordering is observed for different PEG lengths (20KC10 vs 10KC10 in Figure 10). Systems having shorter PEG chains order more distinctively (sharper peak) compared to system having longer PEG chains. In addition, for the same PEG midblock, somewhat better ordering is observed

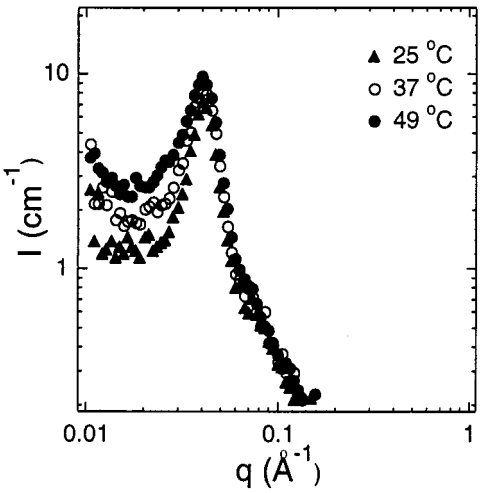

Figure 9. SANS pattern of 10KC8 12 wt % as a function of temperature.

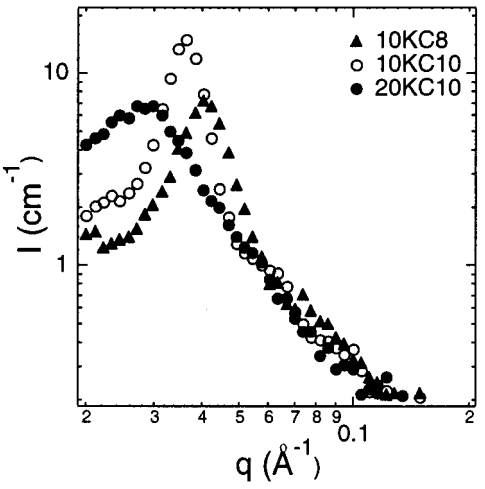

Figure 10. Comparison of SANS patterns for various species at fixed concentration (12 wt % at 25 °C).

for systems with longer end group lengths (10KC10 vs 10KC8 in Figure 10).

Aggregation Number of the Hydrophobic Core. To estimate the aggregation number of the hydrophobic cores from the SANS data, it is necessary to know what ordered structure is formed (bcc, fcc, or sc). A 15 wt % solution of 10KC10 reveals small second- and third-order peaks at $\sqrt{2}$ and $\sqrt{3}$ positions relative to the primary peak. Similarly, a 15 wt % solution of 6KC8 and a 17 wt % of 10KC8 show small peaks at $\sqrt{2}$ and $\sqrt{3}$ positions relative to the primary peak (Figure 11). These higher-order peaks exclude the possibility of an fcc structure. The simple cubic (sc) structure is considered very unlikely, since a variety of experimental and theoretical studies of colloidal crystallization have found fcc and/or bcc structures in most cases.[25−36] Therefore, we assign a bcc structure and compute N_{ag} as the number of hydrophobes in each core:[45] the number concentration of hydrophobe is known and divided by the number density of hydrophobic cores in the bcc structure, $q_{max}^3/(\pi\sqrt{32})$, where q_{max} is q at the primary peak (Table 3). In addition, N_{ag} was also estimated from the extrapolated absolute intensities at $q \rightarrow 0$ ($I(q\rightarrow 0)$) of dilute (0.5 wt %) solutions of monofunctional R_f-PEGs. Using the correlation that $I(q\rightarrow 0) = n(\phi)(\Delta\rho)^2 v^2$, where $n(\phi)$ is the number density of particles, $\Delta\rho$ is the excess scattering length density of the R_f-PEGs with respect

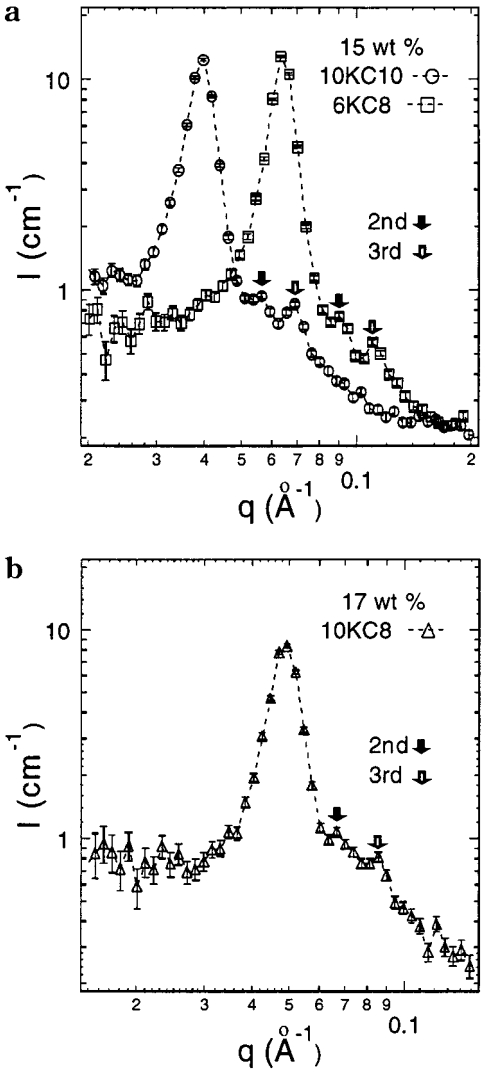

Figure 11. SANS pattern of R_f-PEG showing higher order peaks at 25 °C: (a) 15 wt % solution of 10KC10 and 6KC8 and (b) 17 wt % solution of 10KC8.

Table 3. Aggregation Number of R_f-PEG Solutions Estimated from SANS

species	concn (wt %)	agg no.[a]	species	concn (wt %)	agg no.[a]
6KC8	15	32 ± 4	10KC10	15	45 ± 6
10KC8	8	32 ± 4	20KC10	12	51 ± 9
10KC8	12	32 ± 4	5KmPC8	0.5	28 ± 4
10KC8	17	34 ± 4	5KmPC10	0.5	44 ± 5
10KC10	12	50 ± 6			

[a] Determined from SANS (see text).

to D_2O, and v is the dry volume of an aggregate,[19] the aggregation numbers were estimated from these $I(q\rightarrow 0)$ values. The results for dilute micelles coincide well with the aggregation numbers inferred from ordered gels based on a bcc structure assignment (Table 3). Neither concentration (8−17 wt % for 10KC8 and 0.5 wt % for 5KmPC8; 12−15 wt % for 10KC10, and 0.5 wt % for 5KmPC10) nor temperature (25−49 °C for 10KC8 in Figure 9) affects the aggregation number. Furthermore, N_{ag} is not affected (within experimental uncertainty) by substantial changes in PEG length (C8 with 6K or 10K here or 35K in ref 6; C10 with 10K or 20K) or topology (dangling ends vs loops: 5KmPC8 vs 10KC8; 5KmPC10 vs 10KC10). Thus, the hydrophobe length governs the aggregation number, similar to the case of poly(butylene

oxide)−poly(ethylene oxide) triblock copolymer solutions.[46]

Discussion

Here we provide an integrated view of the rheological and structural properties of these associating polymers and their implications for theory. The rheology of the R_f-PEGs that exhibit single-phase behavior reflects the progression of network topology with concentration established for associative thickners.[6−10,19−21] In contrast, the R_f-PEG systems that exhibit sol−gel equilibrium show pronounced effects of micelle−micelle packing in their structure and rheology, which are reminiscent of colloids and micelles but have not been treated previously for hydrophobically modified PEG. Micelle−micelle repulsion drives ordering at concentrations above but near their equilibrium gel concentration and enhances the elastic moduli of their disordered gels.

Characteristics of Single-Phase Species. Annable has developed a quantitative model of the topology of end-associating polymer solutions which predicts the G_∞ and relaxation time as functions of concentration.[10] The key features of the model are accounting for the continuous change in network topology with increasing concentration: at low concentration, the polymers exist in isolated flowerlike micelles, and as concentration increases, these form clusters that grow until one cluster spans the whole system, forming a very soft gel. In this initial gel, many micelles only have functionality 2 in terms of their connection to other micelles; the network junctions (micelles with functionality 3 or higher) are spanned by chains of flowerlike micelles, called "superbridges".[9,10] With further increase in concentration, the average distance between micelle cores decreases, and the probability of forming direct bridges from micelle-to-micelle increases; consequently, the average functionality increases, and the length of the superbridges decreases as concentration increases until all bridges are direct, single-chain connections.[4−10,17−21]

Although the Annable model describes the increase in the plateau modulus (Figure 2a) and relaxation time (Figure 2b) of 20KC10 with concentration of single-phase systems (whether hydrocarbon or fluorocarbon ended), it does not describe them quantitatively. In his model, N_{ag} can be deduced by fitting the model to the profiles of G_∞ and relaxation time vs concentration. However, the aggregation numbers estimated from this model are relatively small (3 or 4 for our single-phase systems and 7 for C16 alkyl-ended PEG[10]) compared to the aggregation numbers observed experimentally (30 or 50 for C8 and C10 fluoroalkyl and between 20 and 40 for C16 alkyl-ended systems[15]). Viewed another way, if the observed N_{ag} were used in the model, the predicted modulus at every concentration is substantially higher than observed, the concentration at which the predicted modulus rises to its saturated value is much lower than observed, and model predictions for the relaxation time are faster than the observed values. All of these discrepancies indicate that the model is biased toward direct bridges relative to the actual systems.

We offer three observations regarding the possible origins of the disparity between the model and experiment. First, the model treats the PEG chains as if they were independent, unperturbed random coils distributed on a random lattice. At low concentration, the real situation consists of dispersed flowerlike micelles that have high PEG concentration in their corona. (Based on the scaling behavior of spherical brushes,[24] the corona for 35K PEG attached to a core with $N_{ag} \approx 40$ has ~5-fold higher concentration than a 35K PEG random coil.) Therefore, the probability of entities being close enough to bridge is lower than anticipated by the Annable model.

Second, the model allows the fraction of bridges to rise from 0 to $^1/_2$ as soon as the average number of cores within the span of one chain reaches two. However, research on block copolymers indicates that even in the limit of bulk polymer (no solvent) the fraction of bridges does not reach $^1/_2$.[47,48] Many random walks originating at a given core do not reach the midpoint with respect to neighboring cores and are more likely to return to the core from which they began: of those that reach the midpoint, half are likely to reach the neighboring core.[49] By neglecting this effect, the Annable model greatly overpredicts the fraction of bridges.

Finally, the Annable model neglects the contribution of micelle−micelle packing to the macroscopic modulus. In addition to the observed ordering transition, evidence of micelle−micelle packing is seen in reported values of modulus that exceed $^1/_2 n\kappa T$ (the factor of $^1/_2$ resulting from the upper limit on the number of chains that form bridging configurations).[10,16] Micelle−micelle packing gives rise to a C^2 increase in modulus (until the excluded-volume interaction becomes screened[50]), which could contribute to the continued rise in the modulus beyond the concentration at which Annable model predicts that the topology of the gel has saturated.

Ordering Transition. The most distinct rheological characteristic of the present sol−gel coexisting species—the appearance of a new elastic plateau in the low-frequency regime (G_L)—has not been reported before for associative polymer solutions. Instead, the abrupt increase in the low-frequency modulus with increasing concentration is reminiscent of the ordering transition of block copolymer solutions,[27,35] verified by the ordering observed using SANS. At concentrations just below the transition, the primary relaxation mechanism is the exchange of end groups from one micelle core to another (called the "end group dissociation mode").[9,10] Physically, this mode is still present in the ordered state (a small drop in G' from G_∞ to G_L provides a remnant signature of this relaxation mode); however, a much slower relaxation process is also present, associated with the much slower process of motion of micelles from one lattice site to another. This very slow relaxation mode also explains the long recovery time after loading and yielding behavior in creep.

The observed effects of temperature and molecular structure on the ordering transition are consistent with this physical picture of a densely packed micelle structure. Because of the LCST behavior of PEG in water, the micelle corona becomes thinner with increasing temperature. At fixed concentration, the average distance between micelle cores remains the same. Thus, with increasing temperature the average repulsion between micelles decreases, which causes a decrease in long-range order. The weaker ordering with increasing temperature (Figure 9) correlates with the decrease in the low-frequency modulus (Figure 6), supporting the hypothesis that the elasticity of the ordered lattice is responsible for the low-frequency plateau. With decreasing length of the PEG midblock for a given end group length (hence, fixed N_{ag} of the hydrophobic core), the corona is thinner and denser; the ordering transition

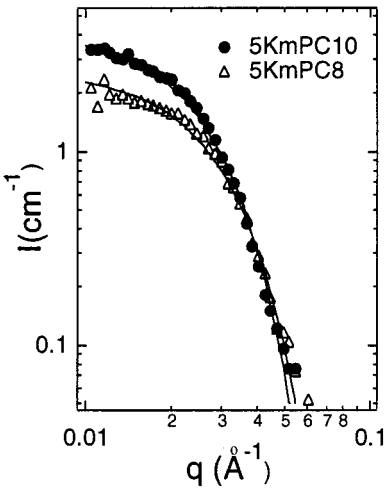

Figure 12. SANS pattern of dilute (0.5 wt %) monofunctional R_f-PEG solutions. Curves show the best fit with the Guinier relation, $I = I(q\rightarrow 0)\exp(-q^2R_G^2/3)$. For 5KmPC10, $I(q\rightarrow 0) \approx 4.1$ cm^{-1}, corresponding to $R_G \approx 70$ Å. For 5KmPC8, $I(q\rightarrow 0) \approx 2.6$ cm^{-1} and $R_G \approx 63$ Å.

shifts to higher weight concentration (similar volume concentration of micelles) and displays stronger long-range order, which correlates with higher low-frequency modulus and greater resistance to creep. With increasing fluoroalkyl length for a fixed PEG length and concentration, the degree of ordering increases, as does the low-frequency modulus and the resistance to creep. These effects are consistent with the increase in aggregation number with increasing fluoroalkyl length (Table 3), making the corona more rigid.[36]

We summarize the phase behavior as a function of molecular structure using a "phase diagram". It is not yet known how to place systems with different structures onto a phase diagram. Unlike block copolymers in which the phase behavior as a function of molecular structure (choice of monomers and chain length) and conditions (T, p) is described using χN, the energetics of interaction in associative polymers are so strong that they are considered to drop out of the problem: the phase behavior is governed by the configurational entropy of the end groups distributing themselves among the hydrophobic cores. Therefore, neither the strength of interaction among the end groups nor the temperature is an appropriate variable for representing the phase behavior. Both the Semenov model and the sticky hard-sphere model suggest that the aggregation number be used as the relevant variable. (At high enough aggregation number the system should exhibit a first-order phase transition from sol to gel.) However, the observed phase behavior shows that at fixed N_{ag} there are dramatic changes in phase behavior depending on PEG length. We highlight the strong effect of PEG length by using it to display the phase behavior for polymers of fixed fluoroalkyl length, corresponding to fixed N_{ag} (Figure 13). It is striking that the two diagrams are very similar to each other (illustrating the surprisingly weak effect of N_{ag} on the phase behavior).

Given that ordering occurs at concentrations just above $C_{gel,eq}$, the phase separation observed in the present systems appears to be closer to a gas−solid-like transition as predicted by Semenov et al.[24] than a gas−liquid transition observed for a longer PEG (35K) with hydrocarbon tails.[15]

Plateau Modulus at High Frequency (G_∞). The theories of rubber elasticity[51] and transient networks

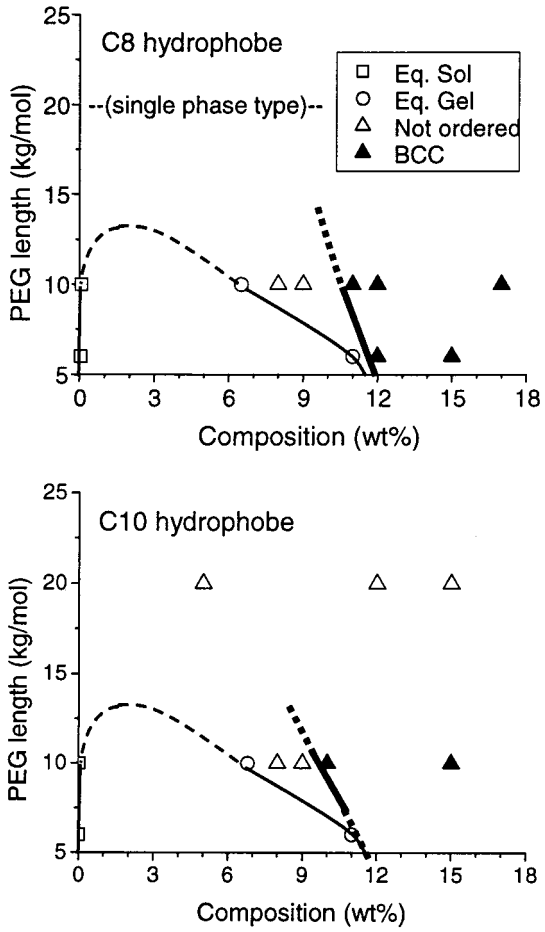

Figure 13. Schematic diagram of phase and ordering behavior of R_f-PEG solutions for a given hydrophobe length in terms of PEG length and concentration. Thin line represents the sol−gel equilibrium boundary, and the thick line represents the ordering transition. Dotted lines illustrate expected trends beyond the range covered by the experimental data.

have been adapted[10] to explain the modulus of the associating polymer system, which says that

$$G_0 = g\nu kT = g\rho RT/M_{e0}$$

where G_0 is the pseudo-equilibrium modulus of the material, ν is the number of network strands per unit volume, ρ is the density of the material, M_e is the apparent molecular weight between cross-links, and g is the correction factor to account for network defects. This correction factor is close to 1 and varies weakly with the functionality of the cross-links.[48] Interchain looping or entanglement tends to increase g, whereas dangling bonds and other network defects tend to decrease g. For an associating polymer solution that is described by the Maxwell model, G_0 corresponds to the plateau value of G' at high frequency (G_∞),[52] assuming that only the entropic elasticity of the chains contributes to the modulus. So, G_0/nkT is an estimate for the fraction of elastically effective chains, where n is the number of polymer chains per unit volume (based on the known concentration and molecular weight). For hydrocarbon-ended systems, this value increases linearly at low concentrations and saturates to ~1 at high concentrations.[10,16] For 20KC10, a single-phase system (Figure 14a), this was also the case. This linear increase of G_0/nkT (or quadratic increase of G_0, Figure 2) with concentration has been observed previously in a number

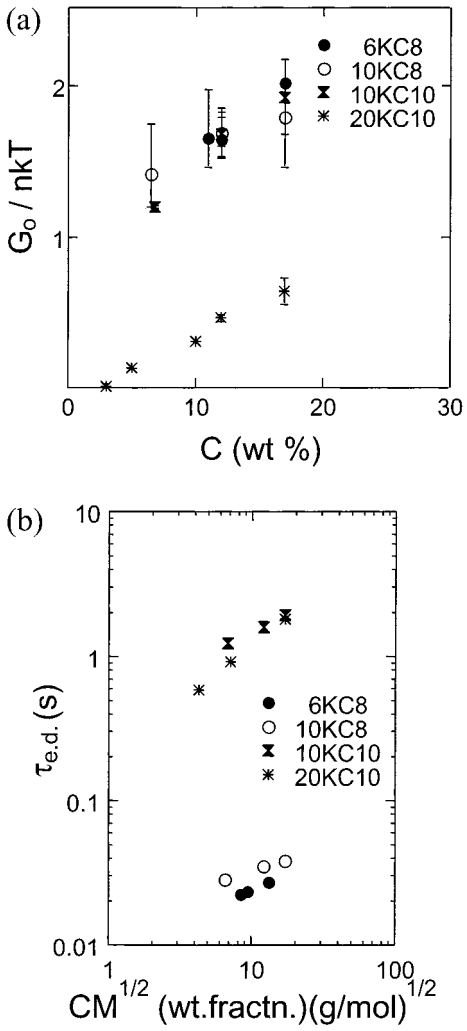

Figure 14. Concentration dependence of the (a) "effective fraction", G_0/nkT, and (b) $\tau_{e.d.}$, where C is concentration (weight fraction) and M is molecular weight. Note that polymers with fixed end group have nearly the same $\tau_{e.d.}$, despite the qualitative difference in their phase behavior (e.g., single-phase 20KC10 vs sol−gel coexistence 10KC10).

of single-phase alkyl-ended PEG systems.[10−13] Two explanations have been offered: the change in superbridge length with concentration[10] or pairwise colloidal interactions.[16]

Interestingly, a much higher concentration is required to reach saturation of G_0/nkT for 20KC10 (no roll-off is evident even at 17 wt %) than for previously reported hydrocarbon-ended systems (roll-off is evident at concentrations below 10 wt % for either 35K or 20K PEG with C16 alkyl ends[10,16]). This difference cannot be explained by a difference in aggregation number, since they are similar (∼50 for 20KC10 compared to ∼40 for C16 alkyl-ended 35K PEG, and greater N_{ag} shifts saturation to lower concentration in Annable's model). Also, at a given concentration (wt %), comparable fluoroalkyl systems show lower G_0/nkT than their alkyl-ended counterparts. A related difference between the phase behavior of fluoroalkyl-ended PEG relative to alkyl-ended PEG has been noted previously: pairs of systems have been identified that have comparable N_{ag} and PEG length, in which the fluoroalkyl-ended system exhibits single-phase behavior and their alkyl-ended analogue shows sol−gel equilibrium. We infer from these three observations that fluoroalkyl-ended systems have a stronger intermicelle repulsive interaction than their alkyl-ended counterparts (with similar N_{ag} and PEG length). An increase in the repulsive part of the intermicelle interaction would disfavor direct bridging in favor of superbridging (hence, the modulus would be lower and the concentration required to drive the system completely to direct bridging would be higher). Similarly, since the entropic attractive term is regulated by N_{ag}, the greater tendency to exhibit sol−gel equilibrium for the alkyl-ended-PEGs suggests that the intermicelle repulsion accounts for the difference (greater for fluoroalkyl-ended PEGs).

In contrast to the small values of G_0/nkT (<1) for single-phase systems, large values of G_0/nkT (>1) are found for the phase-separating species, even near $C_{gel,eq}$ (Figure 14a). When compared at a given concentration above their ordering transitions, 10KC10, 10KC8, and 6KC8 all exhibit similar G_0/nkT at high-frequency (at 17 wt %, $G_0/nkT \sim 1.8$). As previously predicted by Semenov and inferred from observations of $G_0/nkT > 1$ in an alkyl-ended PEG, the high values of G_0/nkT indicate that micelle packing gives a significant contribution to the elasticity of these gels. However, the intermicelle repulsion plays a more pronounced role in the present fluoroalkyl-ended PEGs, which show high values of G_0/nkT for all $C > C_{gel,eq}$ and reach values substantially greater than 1. In contrast, the alkyl-ended system (35K PEG with C18 alkyl ends) only exhibited $G_0/nkT > 1$ at concentrations much greater (∼2×) than $C_{gel,eq}$.[16] This difference may be a consequence of the different PEG lengths used, which significantly alters the phase behavior, apparently causing the 35K PEG with C18 alkyl ends to show gas−liquid-type phase separation (lower $C_{gel,eq}$ with little repulsive interaction) while the R_f-PEGs that show sol−gel coexistence show more gas−solid character (higher $C_{gel,eq}$, close to the ordering transition). In addition, the larger values of G_0/nkT in the present systems may reflect the differences between fluoroalkyl-ended and alkyl-ended systems discussed above: fluoroalkyl-ended systems appear to have stronger intermicelle repulsion than their alkyl-ended counterparts.

End Group Dissociation Mode. When end group dissociation is the predominant relaxation mechanism, $\tau_{e.d.}$ is the single relaxation time[3−21,53] and the fluid is well approximated by a Maxwell fluid (e.g., 20KC10 at all concentrations investigated). The value of $\tau_{e.d.}$ is dominated by the end group length regardless of the phase behavior (Figure 14b). This relaxation time increases with concentration approximately linearly (e.g., up to 17 wt % for 20KC10) for single-phase-type systems and more weakly for species showing phase separation. This reduced dependency of $\tau_{e.d.}$ on concentration for the phase-separating species implies that the topology of the network does not change substantially in this concentration range ($C > C_{gel,eq}$), consistent with the evidence that the micelles are already fairly densely packed.

Conclusions

Despite a number of prior studies of aqueous solutions of PEG modified with hydrophobes at both ends, knowledge regarding the aggregation number of the association site, the most important parameter in theoretical models, is rather limited. This situation arises in part due to uncertainties associated with the methods previously used (fluorescence and intrinsic viscosity).[15] In addition, the effects of molecular parameters have not

been systematically examined. Probing the effects of molecular structure, concentration, and temperature revealed that the aggregation number is dominated by the fluoroalkyl length. In turn, known values of the aggregation number permit meaningful comparison with theory: systems with fixed aggregation number show much wider variations in phase behavior than are compatible with existing models.[15,24]

Although the rheological signature of ordering is well documented in block copolymers, it has not been reported in associative polymer solutions. Here, we observed the development of a low-frequency plateau in addition to the familiar nearly single-relaxation mode of associative polymers. Using neutron scattering, we identify its origin in the transition to a cubic ordered phase. The proximity of the ordering concentration to the equilibrium gel concentration suggests that the present systems have characteristics of a gas−solid transition, as hypothesized by Semenov.[24]

Acknowledgment. This research was supported in part by a grant from NSF (CTS-9729443), a graduate fellowship from the Korean Ministry of Education (Giyoong Tae), and the MRSEC Program of NSF (DMR-0080065). This work benefitted from the use of the IPNS at Argonne National Laboratory (US DoE-BES contract W-31-109-ENG-38).

References and Notes

(1) *Hydrophilic Polymers: Performance with Environmental Acceptability*; Glass, J. E., Ed.; ACS Advances in Chemistry Series 248; American Chemical Society: Washington, DC, 1996; Chapter 10.
(2) *Polymers as Rheology Modifiers*; Schulz, D. N., Glass, J. E., Eds.; ACS Symposium Series 462; American Chemical Society: Washington, DC, 1989.
(3) Rubinstein, M.; Dobrynin, A. V. *Trends Polym. Sci.* **1997**, June, *5* (6), 181.
(4) Menchen, S.; Johnson, B.; Winnik, M. A.; Xu, B. *Chem. Mater.* **1996**, *8*, 2205.
(5) Menchen, S.; Johnson, B.; Winnik, M. A.; Xu, B. *Electrophoresis* **1996**, *17*, 1451.
(6) Xu, B.; Li, L.; Yekta, A.; Masoumi, A.; Kanagalingam, S.; Winnik, M. A.; Zhang, K.; Macdonald, P. M.; Menchen, S. *Langmuir* **1997**, *13*, 2447.
(7) Xu, B.; Yekta, A.; Li, L.; Maosumi, Z.; Winnik, M. A. *Colloids Surf. A* **1996**, *112*, 239.
(8) Yekta, A.; Xu, B.; Duhamel, J.; Adiwidjaja, H.; Winnik, M. A. *Macromolecules* **1995**, *28*, 956.
(9) Tam, K. C.; Jenkins, R. D.; Winnik, M. A.; Bassett, D. R. *Macromolecules* **1998**, *31*, 4149.
(10) Annable, T.; Buscall, R.; Ettelaie, R. *J. Rheol.* **1993**, *37*, 695.
(11) Jenkins, R. D.; Silebi, C. A.; El-Asser, M. A. *Polym. Mater. Sci. Eng.* **1989**, 629.
(12) Kaczmarski, J. P.; Glass, J. E. *Macromolecules* **1993**, *26*, 5149.
(13) Lundberg, D. J.; Brown, R. G.; Glass, J. E.; Eley, R. R. *Langmuir* **1994**, *10*, 3027.
(14) Pham, Q. T.; Russel, W. B.; Lau, W. *J. Rheol.* **1998**, *42*, 159.
(15) Pham, Q. T.; Russel, W. B.; Thibeault, J. C.; Lau, W. *Macromolecules* **1999**, *32*, 2996.
(16) Pham, Q. T.; Russel, W. B.; Thibeault, J. C.; Lau, W. *Macromolecules* **1999**, *32*, 5139.
(17) Francois, J.; Maitre, S.; Rawiso, M.; Sarazin, D.; Beinert, G.; Isel, F. *Colloids Surf. A* **1996**, *112*, 251.
(18) Cathebras, N.; Collet, A.; Viguier, M.; Berret, J. *Macromolecules* **1998**, *31*, 1305.
(19) Serero, Y.; Aznar, R.; Porte, G.; Berret, J.-F.; Calvet, D.; Collet, A.; Viguier, M. *PRL* **1998**, *81*, 5584.
(20) Serero, Y.; Jacobson, V.; Berret, J.-F.; May, R. *Macromolecules* **2000**, *33*, 1847.
(21) Berret, J.-F.; Serero, Y.; Winkleman, B.; Calvet, D.; Collect, A.; Viguier, M. *J. Rheol.* **2001**, *45*, 477.
(22) Tae, G.; Kornfield, J. A.; Hubbell, J. A.; HogenEsch, T. E.; Johannsmann, D. *Macromolecules* **2001**, *34*, 6409.
(23) Tae, G.; Kornfield, J. A.; Hubbell, J. A. Manuscript in preparation.
(24) Semenov, A. N.; Joanny, J. F.; Khokhlove, A. R. *Macromolecules* **1995**, *28*, 1066.
(25) McConnel, G. A.; Gast, A. P.; Huang, J. S.; Smith, S. D. *PRL* **1993**, *71*, 2102.
(26) Watanabe, H.; Kotaka, T.; Hashimoto, T.; Shibayama, M.; Kawai, H. *J. Rheol.* **1982**, *26*, 153.
(27) Watanabe, H.; Matsumiya, Y.; Kanaya, T.; Takahashi, Y. *Macromolecules* **2001**, *34*, 6742.
(28) Adams, J. L.; Graessley, W. W.; Register, R. A. *Macromolecules* **1994**, *27*, 6026.
(29) Mortensen, K. *Europhys. Lett.* **1992**, *19*, 599.
(30) Almgren, M.; Brown, W.; Hvidt, S. *Colloid Polym. Sci.* **1995**, *273*, 2.
(31) Pople, J. A.; Hamley, I. W.; Fairclough, J. P. A.; Ryan, A. J.; Yu, G.-E.; Booth, C. *Macromolecules* **1997**, *30*, 5721.
(32) Prud'homme, R. K.; Wu, G.; Schneider, D. K. *Langmuir* **1996**, *12*, 4651.
(33) Mingvanish, W.; Kelarakis, A.; Mai, S.-M.; Daniel, C.; Yang, Z.; Havredaki, V.; Hamley, I. W.; Ryan, A. J.; Booth, C. *J. Phys. Chem. B* **2000**, *104*, 9788.
(34) Kelarakis, A.; Castelletto, V.; Chaibundit, C.; Fundin, J.; Havredaki, V.; Hamley, I. W.; Booth, C. *Langmuir* **2001**, *17*, 4232.
(35) Daniel, C.; Hamley, I. W.; Wilhelm, M.; Mingvanish, W. *Rheol. Acta* **2001**, *40*, 39.
(36) Watzlawek, M.; Likos, C. N.; Lowen, H. *PRL* **1999**, *82*, 5289.
(37) Uchida. S.; Ichimura, A.; Ishizu, K. *J. Colloid Interface Sci.* **1998**, *203*, 153.
(38) Mortensen, K.; Brown, W.; Jorgensen, E. *Macromolecules* **1994**, *27*, 1994.
(39) Zhang, H.; HogenEsch, T. E. *Langmuir* **1998**, *14*, 4977.
(40) Zhang, H. S.; Pan, J.; HogenEsch, T. E. *Macromolecules* **1998**, *31*, 2815.
(41) The dynamic moduli do not extend to sufficiently low frequency to prove that there is no other slower relaxation process than the relaxation time associated with the crossover; however, the creep results show good accord between the zero shear viscosity and the product of the modulus and relaxation time inferred from the dynamic moduli, suggesting that indeed there is no other low-frequency relaxation process.
(42) Jenkins and co-workers have investigated the origin of this high-frequency mode by examining its dependence on temperature (*J. Rheol.* **2000**, *44*, 137); unlike the present system, the aggregation number of their C20-alkyl ends increases with increasing temperature. Therefore, they interpret the "fast process" in terms of a micelle relaxation time that slows with increasing temperature due to the increase in aggregation number. Although the present systems do not show a change in aggregation number with temperature (see SANS results below), the physical origin of the high-frequency mode may be similar. Alternatively, the high-frequency mode may reflect internal conformational modes of the PEG chains or high-frequency dynamics associated with the micelled cores (even if they were not connected).
(43) Paulin, S. E.; Ackerson, J.; Wolfe, M. S. *Phys. Rev. E* **1997**, *55*, 5812.
(44) The results shown in Figure 7 represent those for ∼4 h of recovery from prior flow history; different results might be obtained if even longer annealing were allowed between experiments.
(45) There are two conventions used for the aggregation number. Some define it as "the number of chains per micelle",[15,18] whereas others do as "number of hydrophobes per micelle".[6,7]
(46) Liu, T.; Zhou, Z.; Wu, C.; Nace, V. M.; Chu, B. *Macromolecules* **1997**, *30*, 7624.
(47) Watanabe, H. *Macromolecules* **1995**, *28*, 5006.
(48) Watanabe, H.; Sato, T.; Osaki, K. *Macromolecules* **2000**, *33*, 2545.
(49) Matsen, M. W.; Schik, M. *Macromolecules* **1994**, *27*, 187.
(50) McConell, G. A.; Gast, A. P. *Macromolecules* **1997**, *30*, 435.
(51) Treloar, L. R. G. *The Physics of Rubber Elasticity*, 2nd ed.; 1958.
(52) Roovers, J. *Macromolecules* **1991**, *24*, 5985.
(53) Zhang, K. W.; Xu, B.; Winnik, M. A.; Macdonald, P. M. *J. Phys. Chem.* **1996**, *100*, 9834.

MA011809E